PHOTON CORRELATION SPECTROSCOPY STUDY ON THE STABILITY OF SMALL UNILAMELLAR DPPC VESICLES

E. L. CHANG, B. P. GABER, AND J. P. SHERIDAN
Molecular Optics Section, Optical Probes Branch, Naval Research Laboratory, Washington, D. C. 20375

ABSTRACT The growth in size of dipalmitoylphosphatidylcholine small unilamellar vesicles (SUV) below T_m has been studied by photon correlation spectroscopy and differential scanning calorimetry. We see an initial fast rise of the hydrodynamic diameter of the vesicles followed by a slower increase. We assign the slow component of the size change to fusion of SUV. The order of the kinetics appears to be higher than first order. The estimated half lifetime of the fusion is ~67 h. The diameters for the fast and slow processes at $t = 0$ are 756 and 256 Å, respectively, while as $t \rightarrow \infty$ the diameters increase to 1,570 and 733 Å, respectively.

INTRODUCTION

Aqueous suspensions of pure, saturated chain phospholipid vesicles are often used as a model of the lipid component of plasma membranes. The vesicles are usually formed from aqueous dispersions of lecithin subjected to intense bursts of rapidly fluctuating pressure. The resulting size of the small unilamellar vesicles (SUV) appears to have a lower limit between 200 to 250 Å (Huang, 1969). This limit is a likely consequence of the molecular structure of the amphiphiles coupled with thermodynamic constraints on the surface free energy (Tanford, 1979). A major advantage of SUV is their relative homogeneity when prepared by sonication, and their easily defined surface area and internal volume. However, it is also known (e.g., Suurkuusk, et al., 1976; Tsong and Kanehisa, 1977; Peterson and Chan, 1978; Larrabee, 1979; Schullery et al., 1980; Schmidt et al., 1981; Gaber and Sheridan, 1982) that SUV undergo a spontaneous change in size when incubated below T_m. This proclivity to fuse and/or aggregate complicates the utility of SUV as model membranes. On the other hand, the metastability of these fused vesicles, which are of intermediate size between SUV and the lipid dispersions, could offer a dependable method of preparing vesicles in the size range of 600–700Å.

We present here a study of 1,2-dipalmitoyl-*sn*-glycero-3-phosphorycholine (DPPC) SUV at 23°C (T_m = 37°C) using the techniques of photon correlation spectroscopy (PCS) and differential scanning calorimetry (DSC) to monitor the kinetics of SUV size growth. PCS is a sensitive, quickly performed, light scattering measurement of the hydrodynamic properties of macromolecules in solution (Chu, 1974; Berne and Pecora, 1976). One can usually use a concentration of 0.5 mg/ml or less for SUV experiments and perform a complete measurement for the translational diffusion coefficient in as little as 30 s for an accuracy of several percent. PCS is also very sensitive to the presence of large particles so that the inception of fusion/aggregation can, in theory, be detected with great accuracy. A significant advantage of this light-scattering technique over other methods such as DSC, column chromatography, and chemical assays is its nonperturbing nature, which allows us to monitor the changes throughout time for one particular sample without disturbing the parameters of the experiments.

MATERIALS AND METHODS

Sample Preparation

High purity (acetone-precipitated) DPPC obtained from Avanti Biochemicals, Inc. (Birmingham, AL) was dissolved in chloroform and dried into a film using a Brinkmann rotovapor (Brinkmann Instruments, Inc.; Westbury, NY). The SUV preparation was done as previously described in Gaber and Sheridan (1981). 50 μl from the supernatant of a suspension of SUV that had been spun at 45,000 rpm. (at 60°C) was transferred into a cylindrical scattering cell that had previously been thoroughly rinsed with filtered (0.22 μm) distilled water. 5.5 ml of 60°C aqueous solvent was added to the cell and the sample was allowed to cool slowly to 23°C. The final concentrations of lipids used for the "DSC and PCS" measurements were ≤50 and 0.5 mg/ml, respectively.

Instrumentation

A Spectra-Physics 125 He-Ne laser (6328 Å) (Spectra-Physics, Inc., Santa Clara, CA) was used as the coherent light source. The beam was focused to a diameter of ~50 μm inside the center of a cylindrical sample cell. The angle of collection of the scattered light was defined by a series of pinholes and a collection lens. The signal from the PMT was amplified and fed into a PG 502 Tektronix pulse-generator (Tektronix Inc., Beaverton, OR). The pulse generator acted as a pulse shaper and level translator whose output was correlated by a 48-channel Malvern correlator (Malvern Scientific Corp., New York, NY). The entire system was tested by using polystyrene spheres as monodisperse standards of known size. A scattering angle, θ, of 90° was used for all reported measurements.

Data analysis and storage were done on a 48K bytes Apple II Plus microcomputer system. Data were stored on mini-floppy diskettes and analysis was performed directly on the microcomputer.

A Perkin-Elmer DSC-2 differential scanning calorimeter (Perkin-Elmer Corp., Norwalk, CT) was used for all calorimetric measurements. The samples for DSC scans were sealed with "o" rings in stainless steel pans. The approximate sample size was 25 μl of 5% (wt/vol) lipid suspension. Scans were done on the heating cycle using a scan rate of 2.5°/min. The rate of fusion was calculated by measuring the growth of the peak area above 39°C. Further details are described Gaber and Sheridan (1981).

Data Analysis

The photon-correlation data can be analyzed by a variety of methods, with the choice dependent upon the state of the sample. The treatment of unimodal monodisperse and bimodal monodisperse particle distributions has been extensively reported in the literature (c.f. Chu, 1974). However, there does not appear to be an entirely satisfactory method of treating polydisperse, bimodal (or multi-modal) systems whose detailed distributions are not known. Several recent approaches that are moderately successful in this area are the linear spline (Goll and Stock, 1977), the histogram method (Chu, et al. 1979), and the direct inversion of a Fredholm integral of the first kind (Provencher, 1979; Ostrowsky et al., 1981). These techniques, which presuppose only a minimal knowledge of the size distribution function but a precise knowledge of the scattering factors, seek to fit the distribution of particles to either a linear spline function or a set of histograms. For the spline and the histogram method of Chu et al. (1979), a large number of parameters (around 12 to 14) are used. In addition, the resolution appears to be limited to populations that differ in size by a factor of five or more. For our measurements, the range of sizes does not differ by more than a factor of 3. Neither Provencher's (1979) nor Ostrowsky and co-worker's (1981) methods were available to us at the time this paper was written. Their approach of limiting the number of independent parameters in the histogram for the particle distribution function seems to put the histogram methods on a semi-quantitative level.

We use the methods of single-exponential and square of the sum of two exponentials to fit out PCS data (Fig. 1). The base line was included as an independent parameter to be fitted rather than calculated from the experiment. Bargeron (1974) has found that a least-squares fit of the base is at least as accurate as using an experimentally estimated base line. We also analyzed the PCS data with the cumulants approach (Koppel, 1972) to obtain a rough estimate of the polydispersity of our vesicles. The single-exponential analysis was utilized because the kinetics obtained by this method should be comparable to turbidity measurements done by other workers (e.g., Suurkuusk et al., 1976; Schmidt et al., 1981). Double-exponential analysis has been shown to work well for monodisperse bimodal distributions even when the ratio of the two sizes is only two (Bargeron, 1974); one cannot, of course, obtain any information about the widths of the two populations by this method. A short summary of the methods used here follows.

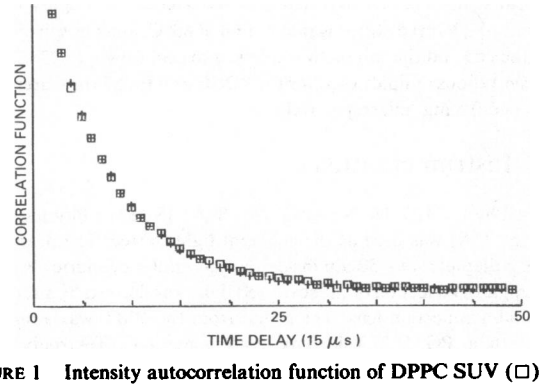

FIGURE 1 Intensity autocorrelation function of DPPC SUV (□) 5 min after reaching 23°C. The data points represent 15-us intervals for a scattering angle of $\theta = 90°$ and incident $\lambda = 6{,}328$ Å. The data are fitted to a single-exponential function (+) with a resulting diffusion coefficient of 1.28×10^{-7} cm^2/s $\pm$ 0.09×10^{-7} cm^2/s. The resolution of the plot is 280 × 160 points.

The correlation function obtained by PCS, for a monodisperse solution where the scattered coherent light is dephased only by random translational motion, is a single exponentially decaying function with a characteristic decay time, τ. The diffusion coefficient, D, is related to τ by

$$\tau = \tfrac{1}{2}DK^2 \tag{1}$$

where K is the absolute value of the scattering vector (Berne and Pecora, 1976).

For a polydisperse solution, the measured diffusion coefficient is the intensity weighted, "Z-average" diffusion coefficient, defined as

$$\overline{D} = \sum_n P_n(\theta)C_nM_nD_n / \sum_n P_n(\theta)C_nM_n. \tag{2}$$

$P_n(\theta)$ is the structure factor for scatterer n, C_n the solute concentration (gm/ml) of species n, and M_n the molecular weight of n.

In the case of a bi-modal distribution, one may analyze the intensity autocorrelation function, $\langle I(0)I(t)\rangle$, as a square of the sum of two exponentially decaying terms, e.g.,

$$\langle I(0)I(t)\rangle = [I_1(0)e^{-t/t_1} + I_2(0)e^{-t/t_2}]^2 + B, \tag{3}$$

where $I_1(0)$, $I_2(0)$, B, t, and t_2 are all parameters to be determined in a nonlinear least-squares analysis. The angular brackets denote an ensemble average. This factoring works best for decay times t_1 and t_2 that are well separated.

For the general case, one may either fit the correlation function to a single exponential (keeping in mind that the diffusion coefficient is the "Z-average" value as defined in Eq. 2) or one may use the cumulants method (Koppel, 1972; Selser et al., 1976) to obtain the various moments of the distribution.

The form of the equation obtained by the cumulants approach is

$$y = -2\overline{\Gamma}t + \{(\Gamma - \overline{\Gamma})^2\}t^2 - \{(\Gamma - \overline{\Gamma}^3\}t^3/3 + \ldots \tag{4}$$

where y is the natural log of the normalized correlation function and $\Gamma = \frac{1}{2}\tau$. Then $D = \Gamma/K^2$ is the Z-average diffusion coefficient, and $\sqrt{\{(\Gamma - \overline{\Gamma})^2\}}/\Gamma^2$ is a measure of the polydispersity, i.e., the ratio of the half-width at half-height to the average value of the distribution. The curly brackets denote an average over a distribution of decay times. There are two disadvantages to this method. The moments are ambiguous for the case of a bi-modal distribution (c.f. Briggs and Nicoli, 1980) and the normalization can be sensitive to the choice of the base line. In this report, we use the value of the base line obtained from the double exponential analysis for normalizing the correlation function and cut off all data beyond and including the first data point at which the difference between the correlation function and the base is zero. The cumulants method is mainly used to obtain a rough estimate of the polydispersity.

In addition to monitoring the growth of the diameters, one can also estimate the relative concentrations of any two species in solution that have widely differing decay times. The procedure is to calculate, from Eq. 3, the scattered intensities, $I_1(0)$, and $I_2(0)$, using a nonlinear least-squares double-exponential fit.

The average scattered intensity from a vertically polarized light beam is proportional to

$$I_n \propto M_nC_nP_n(\theta). \tag{5}$$

Thus, the relative concentration, C_1/C_2, is equal to

$$C_1/C_2 = I_1(0)M_2P_2(\theta)/I_2(0)M_1P_1(\theta). \quad (6)$$

For purposes of relating the PCS results to the kinetics of size growth, where the concentrations of different species (n-mers) vary as a function of time, we may write

$$\bar{d}(t)^{-1} = \sum_n C_n(t)P_n(\theta)M_n d^{-1} / \sum_n C_n(t)P_n(\theta)M_n \quad (7)$$

where $\bar{d}(t)$, the Z-average hydrodynamic diameter at time t, not to be confused with D, the diffusion coefficient, is related to $D(t)$ by the Stokes-Einstein equation

$$\bar{d}(t) = kt/3\pi\eta\bar{D}(t). \quad (8)$$

For one possible model where monomers add to $(n\text{-}1)$-mers to form n-mers, we have

$$M_n/M_1 = n \quad (9a)$$

$$d_n/d_1 = \sqrt{n} \quad (9b)$$

then

$$\bar{d}(t) = d_1\sum_n nP_n(\theta)C_n(t) / \sum_n P_n(\theta)C_n(t)\sqrt{n}. \quad (10)$$

RESULTS

Single Exponential Analysis

The values of the diameter of DPPC SUV below T_m, as determined by single exponential analysis, changed from 325 to ~850 Å in a period of 200 h. The seemingly large value for the initial diameter is, as we shall see, due to the presence of aggregates that form immediately. The hydrodynamic diameters obtained are plotted as a function of time in Fig. 2. The data are characterized by a rapid growth in $d(t)$ followed by a much slower size change implying that at least two processes are occurring. A series of combinations of first and second-order kinetic equations were phenomenologically fitted to the data. It was found that the best fit was a sum of two second-order rate equations of the form

$$d(t) = d(0) + A_1t/(1 + A_2t) + A_3t/(1 + A_4t). \quad (11)$$

One should not attach too much significance to the goodness of the fit and the kinetic order of the above equation. However, Eq. 11 is useful in estimating the time scales of the fast rising portion of the data vs. the slower growing plateau region. The half-lifetimes ($t_{1/2}$) obtained are 2.3 and 57 h, respectively, for A_2^{-1} and A_4^{-1}.

Double Exponential Analysis

The results of fitting the correlation function to a double-exponential form of Eq. 3 are plotted in Fig 3. In all cases, the variances for the double-exponential fit were lower than those for the corresponding single-decay analysis. Although no global minimum can be guaranteed, the double-exponential program always converged to the same value from different starting points in parameter space.

An inspection of Fig. 3 shows that the rate-of-growth of the larger sized population (curve I) is much more rapid than that of the smaller sized population (curve II). For the sake of comparing the characteristic decay times of the two curves in Fig. 3 with then single-exponential results, curves I and II were each fitted to a second-order rate equation. The estimated $t_{1/2}$ obtained were ~18 and ~67 h for I and II, respectively. The diameters at $t = 0$, $d(0)$, were 765 and 266 Å while the $d(\infty)$ were 1570 and 733 Å, respectively.

The relative concentrations of I and II may be estimated by taking the ratio of M_2 to M_1 in Eq. 6 to be approximately equal to the square of the respective radii, e.g.,

$$M_2/M_1 \simeq r_2^2/r_1^2 \quad (12)$$

this approximation is good for large unilamellar vesicles

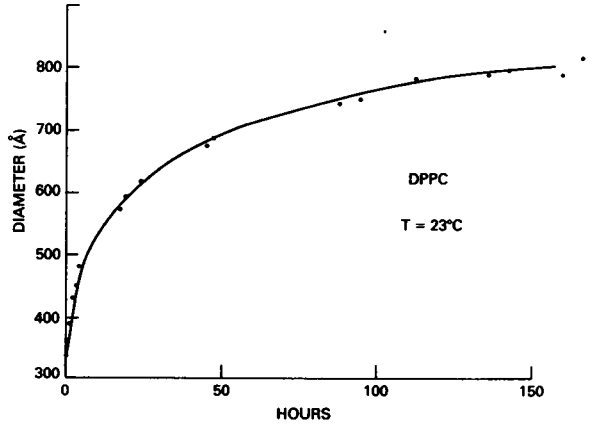

FIGURE 2 Increase in the diameter of DPPC vesicles vs. hours for single-exponential analysis is plotted with the fitted curve from a sum of two second order-like rate equations (see text).

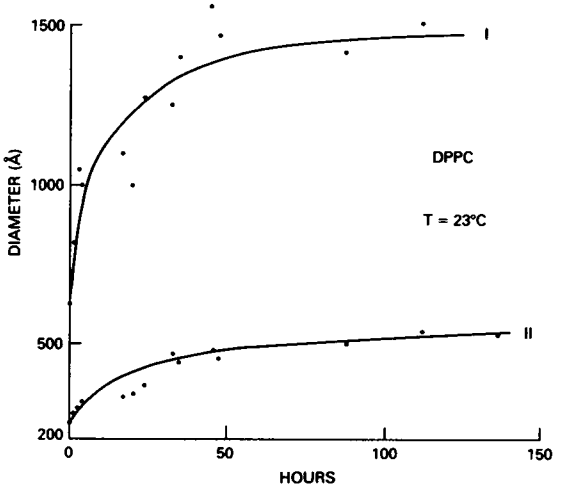

FIGURE 3 Increase in the sizes of the two populations of DPPC vesicles vs. hours for the double-exponential analysis is plotted with curves fitted from two second order-like equations (see text).

but is not as suitable for SUV or nonunilamellar structures.

If we assume, in addition, the scatterers are hollow, spherical shells with isotropic scattering elements, we can use (Oster and Riley, 1952; Tinker, 1972)

$$P_{x,1}(\theta) = \{3(\sin x - \sin x1 - x\cos x + x1\cos x1) / x^3(1 - 1^3)\}^2 \quad (13)$$

for the structure factor, where $x = KR$ is the product of the scattering vector time the outer radius and $1 = a/R$ is the ratio of the inner to outer radius. Using Eq. 6 with the above approximations we estimate that the percentage of I with respect to II increases from ~6% at $t = 0$ to 17% as $t \rightarrow \infty$.

It should be emphasized that the diameters quoted here are obtained from the Stokes-Einstein relation in conjunction with Stokes formula for the friction coefficient of a sphere. In the case of aggregation, the Stokes diameter is related in a complicated manner to the actual physical size of the aggregates. If one assumes, for example, that aggregates are composed of close-packed SUV then the Stokes diameter for a 19-mer SUV aggregate is 642 Å, as obtained by the Kirkwood-Riseman approximation (Yamakawa, 1971).

Cumulants

The polydispersity of the suspension was calculated using the definition given earlier. We found that the polydispersity increased from 0.28 to 0.60 within 40 h then decreased to ~0.44 after 100 h. Although given that there is a bimodal distribution of particles which makes the interpretation of the polydispersity difficult, the result is consistent with the view that at some "midrange" in the fusion aggregation process there should be a myriad of particle sizes, while at either the beginning or end only a few sizes should predominate.

DSC

An aliquot from the same stock preparation of DPPC was taken for DSC measurements. The increase in the peak area above 39°C is plotted in Fig. 4 as a function of time. No fast process can be detected. The DSC data is consistent with the behavior of curve II. The half-lifetime for Fig. 4 is about 45 h as compared with 67 h for curve II. The relatively shorter lifetime for DSC measurements with respect to PCS data can be rationalized as a weak dependence of the size growth of curve II on lipid concentration.

DISCUSSION

We have seen that the change in the overall size of the SUV population follows at least a bi-phasic time dependence. The relatively fast growth of curve I is charting the time course of aggregation (Schmidt et al., 1981), but we cannot determine whether fusion also occurs within these

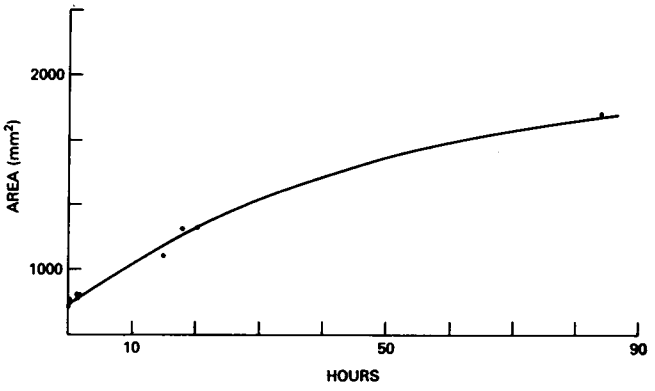

FIGURE 4 DSC of DPPC. The area of the main transition above 39°C (312°K) is plotted against time in hours.

aggregates. The only comment we can offer is that if fusion does occur in these aggregates of SUV, it will most likely not contribute in a direct manner to the growth of curve II. For example, on the basis of a Kirkwood-Riseman calculation (Yamakawa, 1971), we can estimate that the Stokes diameter for a face-centered cubic close-packing model of a 19-mer aggregate is less than that for a 19-mer fused vesicle (~650 vs. ~750 Å). This result is not surprising since a sphere has a high volume-to-surface ratio. Thus if the n SUV of a n-mer aggregate were to all fuse into a single, unilamellar, vesicle, the measured size of this fused vesicle would be larger than the original aggregate. Since curve I is already above curve II in Fig. 3, we can conclude that it is not possible for the aggregates to feed curve II by the direct wholesale fusion of all the monomeric units in a n-mer aggregate. There is still a possibility, however, for curve I to contribute to curve II if only some of the monomeric units in the aggregate fuse then break off to form a separate moiety.

The final size of 733 Å and the slow kinetics of curve II is in good agreement with the results of other studies on the fusion of DPPC SUV (Schullery et al., 1980; Schmidt et al., 1981). For example, Schullery et al. (1980) have found by electron microscopy and column chromatography that after approximately 200 h the fused vesicles have a peak in the size distribution around 700 Å. Schmidt et al. (1981), using turbidity and NMR found that aggregation and fusion occur on distinctly different time scales with the fusion process being second order for part of the size transformation. Our measurements with PCS and DSC concur that fusion does not follow pure first-order or second-order kinetics. Thus, while a binary collisional model can account for some of the kinetic development of the spontaneous fusion of small unilamellar vesicles, a full description would need the inclusion of other mechanisms as well, such as the free diffusion of lipids, and the role of aggregation in fusion.

In summary, we have found that the increase in overall particle size below T_m of a suspension of SUV follow at least a bimodal distribution, each with its own distinct $t_{1/2}$.

The slower growing population, which ultimately reached an average diameter of 733 Å, is identified with the fusion of vesicles while the more rapidly increasing population is thought to consist of aggregates of vesicles. By comparing the $t_{1/2}$ of the fused vesicles with DSC data, we have found that the fusion of SUV depends weakly on the vesicle concentration.

Received for publication 7 January 1981 and in revised form 2 February 1982.

REFERENCES

Bargeron, C. B. 1974. Analysis of intensity correlation spectra of mixtures of polystyrene latex spheres: a comparison of direct least squares fitting with the method of cumulants. *J. Chem. Phys.* 60:2516–2519.

Berne, B. J., and R. Pecora. 1976. Dynamic Light Scattering. John Wiley & Sons, New York.

Briggs, J., and D. F. Nicoli, 1980. Photon correlation spectroscopy of polydisperse systems. *J. Chem. Phys.* 72:6024–6030.

Chu, B. 1974. Laser Light Scattering. Academic Press, Inc., New York.

Chu, B., E. Gulari, and E. Gulari. 1979. Photon correlation measurements of colloidal size distributions. II. Details of histogram approach and comparison of methods of data analysis. *Physica Scripta.* 19:476–485.

Gaber, B. P., and J. P. Sheridan. 1982. Kinetic and thermodynamic studies of the fusion of small unilamellar phospholipid vesicles. *Biochim. Biophys. Acta.* 685:87–93.

Goll, J. H., and G. B. Stock. 1977. Determination by photon correlation spectroscopy of particle size distributions in lipid vesicle suspensions. *Biophys. J.* 19:265–273.

Huang C. 1969. Studies on phosphatidylcholine vesicles formation and physical characteristics. *Biochemistry.* 8:344–354.

Koppel, D. E. 1972. Analysis of macromolecular polydispersity in intensity correlation spectroscopy: the method of cumulants. *J. Chem. Phys.* 57:4814–4820.

Larrabee, A. L. 1979. Time dependent changes in the size distribution of distearoylphosphatidylcholine vesicles. *Biochemistry.* 18:3321–3326.

Oster, G., and D. P. Riley. 1952. Scattering from isotropic colloidal and macromolecular systems. *Acta Crystallogr.* 5:1–6.

Ostrowsky, N., D. Sornette, P. Parker, and E. R. Pike. 1981. Exponential sampling method for light scattering polydispersity analysis. *Optica Acta.* 28:1059–1070.

Peterson, N.O., and S. I. Chan. 1978. The effects of the thermal prephase transition and salts on the coagulation and flocculation of phosphatidylcholine bilayer vesicles. *Biochim. Biophys. Acta.* 509:111–128.

Provencher, S. W. 1979. Inverse problems in polymer characterization: direct analysis of polydispersity with photon correlation spectroscopy. *Makromol. Chem.* 180:201–209.

Schmidt, C. F., D. Lichtenberg, and T. E. Thompson. 1981. Vesicle-vesicle interactions in sonicated dispersions of dipalmitoylphosphatidylcholine. *Biochemistry.* 20:4792–4797.

Schullery, S. E., C. F. Schmidt, P. Felgner, T. W. Tillack, and T. E. Thompson. 1980. Fusion of dipalmitoylphosphatidylcholine vesicles. *Biochemistry.* 19:3919–3923.

Selser, J. C., Y. Yeh, and R. J. Baskin. 1976. A light scattering characterization of membrane vesicles. *Biophys. J.* 16:337–356.

Suurkuusk, J., B. R. Lentz, Y. Barenholz, R. L. Biltonen, and T. E. Thompson. 1976. A calorimetric and fluorescent probe study of gel-liquid crystalline phase transition in small, single lamellar DPPC vesicles. *Biochemistry.* 15:1393–1401.

Tanford, C. 1979. Hydrostatic pressure in small phospholipid vesicles. *Proc. Natl. Acad. Sci. U.S.A.* 76:3318–3319.

Tinker, D. O. 1972. Light scatterikng by phospholipid dispersions: theory of light scattering by hollow spherical particles. *Chem. Phys. Lipids.* 8:230–257.

Tsong, T. Y., and M. I. Kanehisa. 1977. Relaxation phenomena in aqueous dispersions of synthetic lecithins. *Biochemistry.* 16:2674–2680.

Yamakawa, H. 1971. Modern Theory of Polymer Solutions. Harper and Row, New York.